BNL-NUREG--34502

DE84 010891

BNL-NUREG-34502

CONF-840647--15

STRUCTURAL RELIABILITY ANALYSIS AND SEISMIC RISK ASSESSMENT

H. Hwang and M. Reich
Structural Analysis Division
Department of Nuclear Energy
Brookhaven National Laboratory
Upton, NY 11973

M. Shinozuka
Department of Civil Engineering and Engineering Mechanics
Columbia University
New York, NY 10027

ABSTRACT

This paper presents a reliability analysis method for safety evaluation of nuclear structures. By utilizing this method, it is possible to estimate the limit state probability in the lifetime of structures and to generate analytically the fragility curves for PRA studies.

The earthquake ground acceleration, in this approach, is represented by a segment of stationary Gaussian process with a zero mean and a Kanai-Tajimi Spectrum. All possible seismic hazard at a site represented by a hazard curve is also taken into consideration. Furthermore, the limit state of a structure is analytically defined and the corresponding limit state surface is then established. Finally, the fragility curve is generated and the limit state probability is evaluated.

In this paper, using a realistic reinforced concrete containment as an example, results of the reliability analysis of the containment subjected to dead load, live load and ground earthquake acceleration are presented and a fragility curve for PRA studies is also constructed.

INTRODUCTION

Probabilistic risk assessment (PRA) is becoming an important tool for safety evaluation of nuclear power plants. Previous PRA studies such as WASH-1400 (1) mainly concentrated on internal events. Recently, the method has been extended to deal with external events, in particular, the seismic event. As a result of some recent PRA studies such as those carried out for the Zion and Indian Point nuclear power plants (2,3), it was concluded that the seismic event could be a dominant contributor to the risk. The major steps in performing a PRA study are as follows: (1) hazard analysis, (2) response analysis and fragility determination, (3) plant system evaluation and (4) consequence evaluation. It is recognized that all of the above steps involve uncertainties.

For evaluation of structural fragility, the approach used in industrial PRA studies is primarily based on subjective judgements. The main features in the approach are (1) an assumption of lognormal distributions for all variables and (2) a multiplication scheme to predict a median value of a total safety factor which is obtained from the product of many individual safety factors to be determined subjectively. Use of the lognormal distributions for all variables is purely for mathematical expedience. Furthermore, the subjective inputs and multiplication scheme do not appear to be a good combination, since the combination produces fragility curves which are quite sensitive to the subjective inputs. Consequently, fragility curves estimated by different groups of engineers may vary considerably, and the final PRA results are indeed open to question. An alternate approach to the Industrial PRA method is to evaluate the structural response and fragility analytically on the basis of the probabilistic structural mechanics.

In recent years a probability-based reliability analysis methodology for nuclear structures has been developed by the Structural Analysis Division of Brookhaven National Laboratory (BNL)(4-7). An important feature of this methodology is that the finite element analysis and random vibration theory have been incorporated into the reliability analysis. By utilizing this method, it is possible to evaluate the safety margins of nuclear structures under various static and dynamic loads and to generate the structural fragility curves for PRA studies. In this paper, the probability-based reliability analysis method is illustrated by using a realistic reinforced concrete containment structure as an example. The results of the reliability analysis and the corresponding fragility curve are presented.

CONTAINMENT DESCRIPTION

The reinforced concrete containment structure, as shown in Fig. 1, represents a realistic containment in the U.S. The containment consists of a circular cylindrical wall with a hemispherical dome on the top. The dome-cylinder system is fixed at the base. The dimensions of the containment are also shown in Fig. 1. The thickness of the dome is equal to 2'-6" (0.76m) whereas the thickness of the cylindrical wall is 3'-0"

(0.92m). The inside radius of the dome and the cylindrical wall is 62'-0" (18.91m). The height of the cylindrical wall is 150'-6" (45.90m) and the total height of the containment is 215'-0" (65.78m).

The containment wall is reinforced with hoop, meridional and diagonal rebars. The details of rebar arrangement for cylinder and dome of the containment are tabulated in Tables 1 and 2, respectively. The diagonal rebars and steel liners are disregarded in the analysis. Other complications such as penetrations, personal lock and equipment hatches are also not included in the study.

In this paper, the mean values of material properties are used in the analysis. The variations of material properties will be included in the sensitivity study in future. The properties of the concrete and rebars are summarized as follows:

Concrete

The minimum compressive strength of concrete at 28 days is specified as 4000 psi (27.6MPa). However, the mean value is estimated to be 6085.6 psi (42MPa) from test data (8). The weight density of the concrete is taken to be 150 lb/ft^3 (23.55kN/m^3). Young's modulus and Poisson's ratio are 3.6×10^6 psi (24840MPa) and 0.2, respectively.

Reinforcing Bars

As can be seen from Tables 1 and 2, No. 18 rebars are the main reinforcement used in the containment structures. Hence, the statistics for No. 18 rebars are used to represent all other types of rebars. Young's modulus, E_s, and Poisson's ratio are taken to be 29.0×10^6 psi (200100MPa) and 0.3, respectively. From the test data, the mean value of the yield strength fy is estimated to be 71.1 ksi (490.59MPa) (8).

FINITE ELEMENT ANALYSIS

Finite element analysis is used to obtain the static structural responses and the dynamic characteristics of the structure such as the natural frequencies and the associated mode shapes, etc. In order to utilize the finite element analysis results in computing the limit state probabilities, the containment modelling should be made in such a way that the local coordinates of the elements have the same directions as those of the rebars. The finite element utilized in the analysis is the shell element as described in the SAPV computer code. A three-dimensional finite element model is used for the structural analysis of the containment. A detailed cross-sectional view of the containment model is shown in Fig. 2. As can be seen from this figure, the containment is divided into 20 layers. Except for the top layer of the dome, each layer has 24 elements such that the nodal points are taken every 15° in the circumferential direction. This discretization requires a total of 481 nodes and 468 elements.

For dynamic analysis of structures, modal analysis is employed. Using the model described, the first 20 natural frequencies and corresponding modes are evaluated. It is important to choose the significantly participating modes for the reliability analysis. In this study, only the first and second pairs of bending modes are chosen for the analysis.

PROBABILISTIC REPRESENTATION OF LOADS

A containment structure is subjected to various static and dynamic loads during its lifetime. These loads may be caused by normal operating, environmental and accidental conditions. Since the loads intrinsically involve random and other uncertainties, an appropriate probabilistic model for each load must be established in order to perform reliability analysis. In this paper, only the dead load, live load and earthquake ground acceleration are taken into consideration in the analysis.

Dead Load

The dead load primarily arises from the weights of the containment wall. It may have small variation due to weight density of concrete. In this analysis, dead load is assumed to be deterministic and is equal to the design value, which is computed based on the weight density of reinforced concrete as 150 lb/ft^3 (23.55kN/m^3).

Live Load

Because several floors are connected to the containment structure, some live loads act on the containment at the locations where the floors are connected to the containment. The locations and design values of the corresponding live loads are shown as follows:

Elevation	Live Load (kip/ft) (kN/m)
856'-0" (261m)	0.707 (10.32)
828'-3" (253m)	3.000 (43.80)
803'-3" (245m)	0.940 (13.72)
778'-0" (237m)	1.020 (14.89)
755'-0" (230m)	0.930 (13.58)

It is noted that there are some uncertainties as to the actural magnitude of the live load. For the purpose of the present analysis, however, the live loads are also

Table 1. Cylinder Reinforcement.

Elevation	Hoop (Both Sides)	Meridional	
		Outside	Inside
0 to 20'-0"	1# 18 @ 12"	1#18 @ 12"	2# 18 @ 12"
20'-0" to 150'-6"	1# 18 @ 12"	1#18 @ 12"	1# 18 @ 12"

12" = 0.3048m

Table 2. Dome Reinforcement.

Angle From Spring Line	Hoop		Meridional	
	Outside	Inside	Outside	Inside
0° - 45°	2# 18 @ 12"	2# 14 @ 12"	1# 18 @ 12"	1# 14 @ 12"
45° - 90°	1# 18 @ 12"	1# 14 @ 12"	1# 18 @ 12"	1# 14 @ 12"

12" = 0.3048m

assumed to be deterministic and equal to the design values.

Earthquake Ground Acceleration

The earthquake ground acceleration is assumed to act only along the global x direction. It is further assumed that the ground acceleration can be idealized as a segment of a stationary Gaussian process with mean zero and a Kanai-Tajimi spectrum. The Kanai-Tajimi spectrum has the following expression:

$$S_{\ddot{g}\ddot{g}xx}(\omega) = S_o \frac{1 + 4\xi_g^2(\omega/\omega_g)^2}{[1 - (\omega/\omega_g)^2]^2 + 4\xi_g^2(\omega/\omega_g)^2} \qquad (1)$$

where the parametar S_o represents the intensity of the earthquake and ω_g and ξ_g are the dominant ground frequency and the critical damping, respectively. ω_g and ξ_g depend on the soil conditions of the site. In this study, the values of ω_g and ξ_g in Eq. 1 are determined to be 9π rad/sec and 0.6, respectively. The mean duration μ_{dE} of the earthquake acceleration is assumed to be 10 seconds.

The peak ground acceleration A_1, given an earthquake, is assumed to be $A_1 = P_g\sigma_g$ where P_g is the peak factor and taken to be 3.0 in this study. The standard deviation of the ground acceleration σ_g, computed by integrating the Kanai-Tajimi spectral density function with respect to ω, is as follows:

$$\sigma_g = \sqrt{\pi\ \omega_g\ (\frac{1}{2\xi_g} + 2\xi_g)}\ \sqrt{S_o}\ . \qquad (2)$$

The peak ground acceleration given an earthquake can be re-written as

$$A_1 = \alpha_g\sqrt{S_o}\ ,\quad \text{with}\quad \alpha_g = P_g\sqrt{\pi\ \omega_g\ (\frac{1}{2\xi_g} + 2\xi_g)}\ . \qquad (3)$$

If the earthquake occurs in accordance with the Poisson law at a rate λ_E per year, it is easy to show that the probability distribution $F_A(a)$ of the annual peak ground acceleration A is related to the probability distribution $F_{A_1}(a)$ of A_1 in the following fashion:

$$F_A(a) = \exp[-\lambda_E[1 - F_{A_1}(a)]]$$

or

$$F_{A_1}(a) = 1 + \frac{1}{\lambda_E}\ln F_A(a). \qquad (4)$$

Therefore, if a_o indicates the minimum peak ground acceleration for any ground shaking to be considered as an earthquake, $F_{A_1}(a_o) = 0$ and hence, $\lambda_E = -\ln F_A(a_o)$. Assuming that $F_A(a)$ is of the extreme distribution of Type II, $F_A(a) = \exp[-(a/u)^{-\alpha}]$ with $\alpha = 2.61$ and $u = 0.01$, one finally obtains

$$F_{A_1}(a) = 1 - (a/a_o)^{-\alpha} \qquad a \geq a_o. \qquad (5)$$

Under these conditions, one finds that $\lambda_E = 1.50 \times 10^{-2}$/year for $a_o = 0.05g$. Combining Eqs. 3 and 5 and writing Z for $\sqrt{S_o}$, the probability distribution of Z is

$$F_Z(z) = 1 - (\alpha_g z/a_o)^{-\alpha} \qquad \text{for } z \geq a_o/\alpha_g\ . \qquad (6)$$

The information about the maximum earthquake ground acceleration, a_{max}, which represents the largest earthquake possible to occur at a particular site, is needed in order to determine the limit state probability. In this study, a_{max} is chosen to be equal to 0.71g.

LIMIT STATE

A limit state essentially represents a state of undesirable structural behavior. In general, it will depend on the characteristics of the structures and the loadings that act on the structures. For a particular structural system, it is possible that more than one limit state may be considered. Limit states must also be related to the response quantities obtainable from the selected structural analysis method, e.g., the finite element method adopted in this study.

In this paper, the flexural limit state for the containment is defined as follows: At any time during the service life of the structure, the state of structural response is considered to have reached the limit state if a maximum compressive strain at the extreme fiber of the cross-section is equal to 0.003, while the yielding of rebars is permitted. Based on the above definition of the limit state and the ultimate strength theory of reinforced concrete, for each cross-section of a finite element, a limit state surface can be constructed in terms of the membrane stress and bending moment, which is taken about the center of the cross-section (9). A typical limit state surface is shown in Fig. 3. In this figure, point "a" is determined from a stress state of uniform compression and point "e" from uniform tension. Points "c" and "c'" are the so-called "balanced point", at which a concrete compression strain of 0.003 and a steel tension strain of f_y/E_s are reached simultaneously. Furthermore, lines abc and ab'c' in Fig. 3 represent compression failure and lines cde and c'd'e represent tension failure.

RELIABILITY ANALYSIS

Analytically, the eight straight lines of the limit state surface as shown in Fig. 3 are expressed as follows:

$$R_j = \{A_j\}^T\{\tau^{(e)}\} = 0 \qquad j = 1,2,\ldots,8 \qquad (7)$$

where $\{\tau^{(e)}\}$ is the element stress vector, and R_j and $\{A_j\}$ are constants and constant vectors, respectively. In this paper, the stress vector, $\{\tau^{(e)}\}$, consists of two vectors; $\{\tau^{(e)}\}_o$, and $\{\tau^{(e)}\}_d$. The vector $\{\tau^{(e)}\}_o$ is the stress vector due to dead and live loads and is time-invariant and deterministic based on the assumption of the dead and live loads. The vector $\{\tau^{(e)}\}_d$ is stress vector due to the earthquake acceleration and it can be computed as (4,5).

$$\{\tau^{(e)}\}_d = Z[c^{(e)}]\{v_o\}$$

with

$$[c^{(e)}] = [B^{(e)}]\ [\phi^{(e)}]\ [L_q]. \qquad (8)$$

In this expression, $[B^{(e)}]$ and $[\phi^{(e)}]$ are such that $\{\tau^{(e)}\} = [B^{(e)}]\ \{u^{(e)}\}$ with $\{u^{(e)}\}$ being the element nodal displacement vector and $\{u^{(e)}\} = [\phi^{(e)}]\ \{q\}$ with $\{q\}$ being the generalized coordinate vector, respectively. The vector $\{v_o\}$ is obtained from a linear transformation $\{q_o\} = [L_q]\ \{v_o\}$ such that the covariance matrix $[Vv_ov_o]$ of $\{v_o(t)\}$ becomes $[I_m]$ = mxm identity matrix (m=number of modes considered). The vector $\{q_o\}$ is the generalized coordinate vector when $Z = \sqrt{S_o} = 1\sqrt{in^2/sec^3}$ ($25.38\ \sqrt{mm^2/sec^3}$). Thus, $\{\tau^{(e)}\}$ has the following expression:

$$\{\tau^{(e)}\} = \{\tau^{(e)}\}_o + Z\ [c^{(e)}]\ \{v_o\}. \qquad (9)$$

Substitating Eq. (9) into Eq. (7), one obtains

$$\gamma_j^{(e)} - Z\{n_j^{(e)}\}^T \{v_o\} = 0 \qquad (10)$$

where

$$\{n_j^{(e)}\} = \{\bar{A}_j^{(e)}\}/|\bar{A}_j^{(e)}| \text{ with } \{\bar{A}_j^{(e)}\}^T = \{A_j\}^T c^{(e)}$$

and

$$\gamma_j^{(e)} = (R_j - \{A_j\}^T \{\tau^{(e)}\}_o)/|\bar{A}_j^{(e)}|$$

Let $X_{mj}^{(e)}$ be max $|\{n_j^{(e)}\}^T\{V_o\}|$ in $0 \leq t \leq \mu_{dE}$. According to Ref. 5 and 10, the probability distribution of $X_{mj}^{(e)}$ is given in approximation by

$$F_{X_{mj}^{(e)}}(x) = \exp\{-\nu_{jo}^{(e)}\mu_{dE} \exp(-1/2\, x^2)\}$$
$$= 1 - \nu_{jo}^{(e)}\mu_{dE} \exp(-1/2\, x^2) \qquad (11)$$

in which

$$\nu_{jo}^{(e)} = \frac{1}{2\pi}\sqrt{\sum_{a=1}^{m}\sum_{b=1}^{m} n_{aj}n_{bj}E[\dot{v}_{oa}\dot{v}_{ob}]} \qquad (12)$$

where $x \geq \sqrt{2\ln \nu_{jo}^{(e)}\mu_{dE}}$, and $n_{aj}^{(e)}$ is the a-component of $\{n_j^{(e)}\}$ and $E[\dot{v}_{oa}\dot{v}_{ob}]$ is the a-b component of the covariance matrix $[V_{\dot{v}_o\dot{v}_o}]$ of $\{\dot{v}_o(t)\}$. The conditional limit state probability with respect to line j, $P_j(e)$, is obtained as

$$P_j^{(e)} = Pr\{\gamma_j^{(e)} - ZX_{mj}^{(e)} \leq 0\}. \qquad (13)$$

Assuming the containment will not fail under dead and live loads alone, then $\gamma_j^{(e)}$ is positive and $P_j^{(e)}$ can be evaluated as follows:

$$P_j^{(e)} = \int_{Z_{min}}^{Z_{max}} \nu_{jo}^{(e)}\mu_{dE} \exp[1/2(\gamma_j^{(e)}/z)^2]\, f_Z(z)dz. \qquad (14)$$

Furthermore, the conditional limit state probability of the element, P(e), will be bounded as follows:

$$\max P_j^{(e)} < p(e) < \sum_{j=1}^{8} P_j^{(e)}. \qquad (15)$$

Finally, the unconditional limit state probability, P_f, during the lifetime T years is approximated as:

$$P_f = T\lambda_E P(e). \qquad (16)$$

SYSTEM LIMIT STATE PROBABILITY AND SEISMIC FRAGILITY CURVES

The limit state probability evaluated in the preceding section are those at the critical elements. While the limit state probability of the containment as a whole, called system limit state probability, under a certain load combination is always larger than that of the critical elements, the authors' experience in structural reliability analysis suggests that the difference between the system limit state probability and the limit state probability of the critical elements is tolerable for the type of load-structure system under consideration. Therefore, for the sake of analytical simplicity and computational economy, the present study approximates the system limit state probability by the critical element limit state probability.

In this study, the fragility is defined as the conditional limit state probability given a peak ground acceleration. Hence, referring to Eqs. 11 and 14, the fragility is determined in approximation as:

$$P(A_1) = \max_j \text{ and } (e)\{1-\exp[-\nu_{jo}^{(e)}\mu_{dE} \exp\{-1/2\left(\frac{\alpha\,\gamma_j^{(e)}}{\frac{g}{A_1}}\right)^2\}]\} \qquad (17)$$

NUMERICAL RESULTS

On the basis of the finite element model, limit state, loading conditions and reliability analysis method described in the preceding sections, a reliability analysis of the containment under the combination of dead load, live load and earthquake ground acceleration has been carried out. The limit state is reached as the tensile yielding of meridional rebars in the critical elements 6, 7, 18 and 19. These critical elements are located at the first layer and adjacent to global x-axis. The locations of the critical elements and the manner in which the limit state is reached are obviously consistent with the structural and loading symmetry with respect to the x-axis. The lower and upper bounds of the conditional limit state probability are found to be very close and equal to 1.3×10^{-6}. Finally, the unconditional limit state probability during the lifetime of 40 years is 7.8×10^{-7}.

The fragility curve as a function of A_1 measured in g is presented in Fig. 4 and Table 3 shows the corresponding numerical values. Since all the data used in the analysis are taken to be best estimate values (or mean values), this fragility curve may be interpreted as the mean fragility cure. It can be seen from Table 3, the peak ground acceleration corresponding to the median of the curve is 1.02g.

Table 3. Fragility Curve

A_1 (g)	P (A_1)
0.4	1.81 E-10
0.45	3.75 E-8
0.5	1.77 E-6
0.55	3.14 E-5
0.6	2.83 E-4
0.65	1.58 E-3
0.70	6.24 E-3
0.75	1.89 E-2
0.80	5.65 E-2
0.85	0.11
0.90	0.19
0.95	0.31
1.00	0.44
1.02	0.50
1.05	0.57
1.1	0.70
1.15	0.80
1.20	0.88
1.25	0.93
1.3	0.96
1.35	0.98
1.4	0.99
1.5	1.00

CONCLUDING REMARKS

This paper presents a reliability analysis method for nuclear structures. Although only three loads, i.e., dead load, live load and earthquake ground acceleration are mentioned in the paper, it is noticed that the reliability analysis method can be extended to

include other loads such as accidental pressure, tornado and SRV load. Indeed, this extension has been already made by the Structural Analysis Division of Brookhaven National Laboratory. This reliability analysis method can be used to evaluate the raliability level in the existing structures and it can also be used to develop load combination criteria for design of nuclear structures.

Another application of this reliability analysis method is to construct the fragility curves for PRA studies. Since the fragility curve generated by this approach is based on rigorous applications of probabilistic structural analysis, such a fragility curve would represent conditional limit state probability more objectively and thus enhance the credibility of the PRA results.

The present method essentially uses the frequency domain analysis when dealing with the seismic load. In this respect, it is important to confirm more carefully the validity of the assumed analytical form of the spectral density of the earthquake ground acceleration. The adequacy of the assumption that the acceleration can be idealized as a segment of stationary Gaussian process is, however, generally accepted. The importance of considering variability of some other parameter values is recognized and sensitivity analyses to reinforce and complement the reliability analysis presented here will be carried out in the future.

ACKNOWLEDGEMENTS

The authors wish to express their appreciation to Mr. H. Ashar of the Nuclear Regulatory Commission for his support during various phases of this study.

Thanks are due to Mr. P. Brown and Dr. J. Pires for numerical computation and to Ms. D. Votruba and Ms. J. DePass for the typing of this paper.

REFERENCES

1. U.S. Nuclear Regulatory Commission, "Reactor Safety Study - An Assessment of Accident Risks in U.S. Commerical Nuclear Power Plants", WASH-1400, 1975.

2. Commonsealth Edison Co., IL, "Zion Probabilistic Safety Study", Docket 50295, 1981.

3. Power Authority of the State of New York, "Indian Point Probabilistic Safety Study", Docket 50247, March 1982.

4. Hwang, H., Shinozuka, M., Brown, P. and Reich, M., "Reliability Assessment of Reinforced Concrete Containment Structures", BNL-NUREG-51661, NUREG/CR-3227, February, 1983.

5. Kako, T., Shinozuka, M., Hwang, H. and Reich, M., "FEM-Based Random Vibration Analysis of Nuclear Structures Under Seismic Loading", SMIRT-7 Conference, Paper K 7/2, Chicago, IL, August 22-26, 1983.

6. Shinozuka, M., Kako, T., Hwang, H. and Reich, M., "Development of a Reliability Analysis Method for Category I Structures", SMIRT-7 Conference, Paper M 5/3, Chicago, IL, August 22-26, 1983.

7. Shinozuka, M., Kako, T., Hwang, H., Brown, P. and Reich, M., "Estimation of Structural Reliability Under Combined Loads", SMIRT-7 Conference, Paper M 2/3, Chicago, IL, August 22-26, 1983.

8. Hwang, H., Kao, S. and Reich, M., "Probabilistic Models for Materials Used in a Reinforced Concrete Containment", BNL/NUREG-51618, September, 1982.

9. Chang, M., Brown, P., Kako, T., Hwang, H. "Structural Modeling and Limit State Identification for Reliability Analysis of RC Containment Structures", SMIRT-7 Conference, Paper M 3/2, Chicago, IL, August 22-26, 1983.

10. Shinozuka, M., "Random Processes in Engineering Mechanics", Proceedings of the 5th ASCE EMD Specialty Conference at Purdue University, May 23-25, 1983.

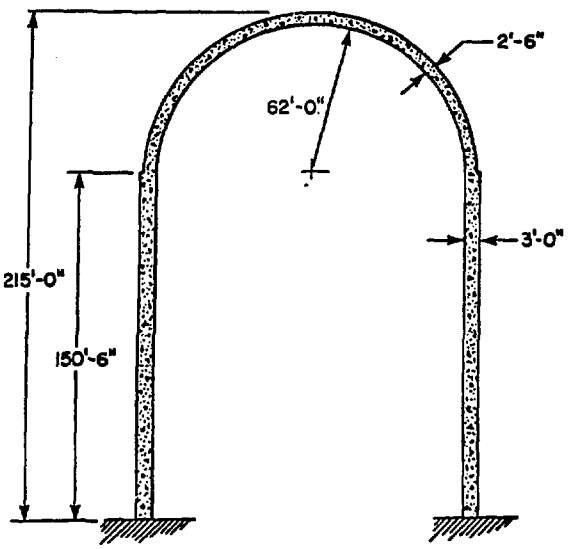

Fig. 1 Containment Structure.

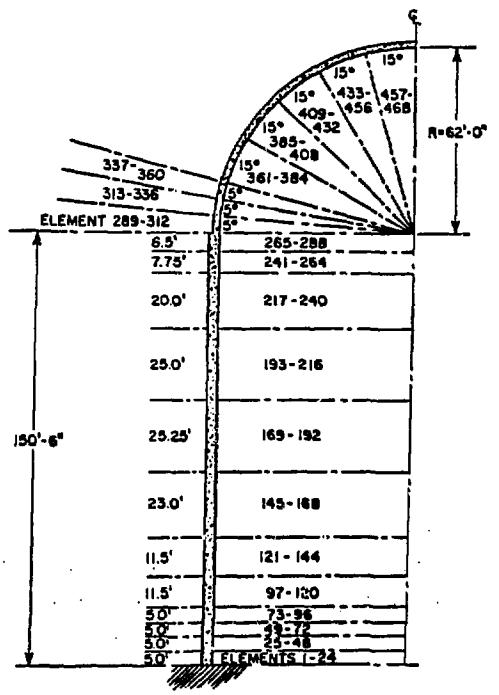

Fig. 2 Cross Section of Containment Model.

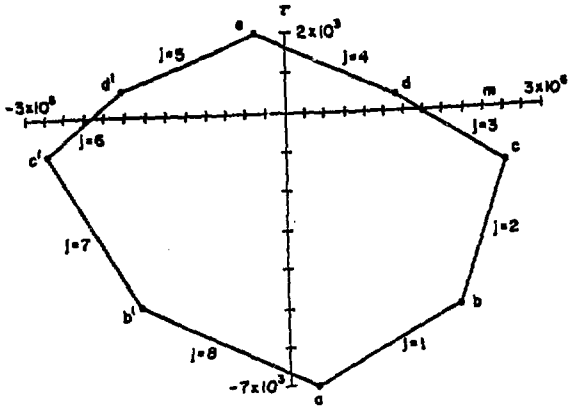

Fig. 3 Limit State Surface.

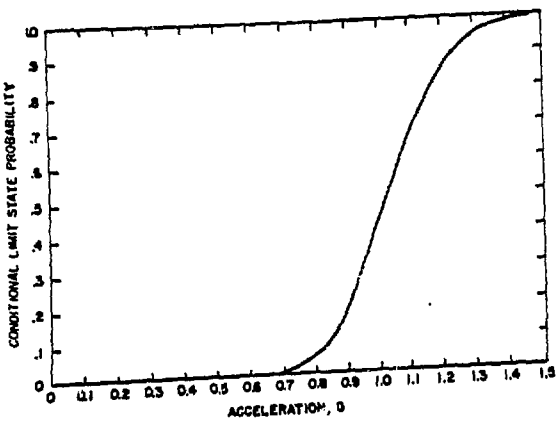

Fig. 4 Fragility Curve.

DISCLAIMER